Myocardial T1 and T2 mapping in diastolic and systolic phase

Abstract The aim of this study was to evaluate the regional (i.e. myocardial segments) variability as well as the overall image quality of cardiac T1 and T2 maps obtained in diastole and in systole. In 22 healthy subjects (group-1), diastolic T1 and T2 maps were obtained at 1.5T in short- axis view at basal, mid-ventricular and apical level, as well as in 4-chamber (4ch) and in 2-chamber (2ch) views. In another group of 25 patients (group-2), the maps were obtained in both diastole and systole. In the group-1, 15.4 % of myocardial segments in T1 maps and 0.8 % of myocardial segments in T2 maps, mainly located at apical level, showed relevant artifacts and/or partial-volume effect and had to be discarded. We found no significant difference in T1 values among basal, mid-ventricular and apical segments. T2 values at apical level were significantly higher than at basal and mid-ventricular level (short-axis, $p \setminus 0.0001$; 4ch, $p \setminus 0.009$; 2ch, $p = 0.0002$ at ANOVA tests). In the group-2, 21.1 %/5.3 % and 4.0 %/0.8 % of segments showed relevant artifacts in diastolic/systolic T1 and T2 maps, respectively. Apical T2 values were significantly lower in systole than in diastole. In systole, there were no significant differences in T1/T2 among basal, mid-ventricular and apical segments. The overall quality of T1 and T2 maps drops in apical segments. This could be problematic when evaluating focal myocardial changes. The acquisition in systole increases the number of evaluable segments.

Keywords T1 mapping · T2 mapping · MOLLI · Left ventricle

Introduction

Recent improvements in cardiac magnetic resonance imaging (CMRI) techniques allow clinically-feasible mapping of myocardial T1 and T2 relaxation times [1–3]. T1 and T2 mapping have shown a better performance than short-time inversion recovery (STIR) and fast spin-echo T2-weighted sequences in identifying edema in myocardial infarction [1, 4–6], myocarditis [7, 8] and Takotsubo cardiomyophaty [9]. T1 mapping techniques, both following contrast administration and pre-contrast (native T1), can quantify diffuse myocardial damage, and in particular diffuse fibrosis [10, 11] and changes resulting from infiltrative processes such as amyloidosis [12–15].

The overall potential of T1 and T2 mapping for identifying myocardial changes is influenced by the accuracy, repeatability and reproducibility of these quantitative techniques. Several studies have addressed these issues and have analyzed pros/cons of the various sequences available to date [16–24], suggesting that T1 and T2 mapping can yield consistent and reproducible results, both in phantom and in vivo.

However, the assessment of the overall quality of T1 and T2 maps in a clinical setting needs further insights. In particular, it is not sufficiently clear whether the obtained T1 and T2 values can depend on the acquisition plane or myocardial segment [17, 24, 25]. These issues are of particular interest when evaluating focal changes, such as myocardial edema, and when aiming to translate the results obtained at group level to the evaluation of single subject, given that they could cause both false positive or false negative results that could impact on patient management.

Furthermore, although T1 and T2 maps are usually acquired in diastole, some pilot studies have shown the feasibility to obtain T1 maps in systole [17, 26, 27].

The aim of this study was to evaluate the overall image quality of cardiac T1 and T2 maps, as well as the variability of the relaxation times among myocardial segments. Accordingly, we obtained diastolic T1 and T2 maps in short and long axes of the left ventricle in 22 healthy subjects (group-1).

Subsequently, in another group of 25 subjects referred at our institution for clinical CMRI examination (group-2), T1 and T2 maps were obtained both in diastole and in systole. This second part of the study was undertaken in order to reduce potential inaccuracies due to partial-volume effect, taking into consideration the results obtained in group-1, and to evaluate the performance of the sequences in a setting closer to the current clinical practice.

Materials and methods

Study population

Group-1

Population of the first part of this study constituted of 22 consecutive healthy asymptomatic subjects (42.3 ± 9.9 years, 3 females, 19 males) without contraindication to MR imaging. All subjects were recruited as control cases for research studies. None were referred as patients for a clinical CMRI scan which then turned out to be normal. None had evidence of cardiovascular disease or cardiac risk factors including hypertension or diabetes. They showed no abnormalities at physical examination, 12-lead ECG and echocardiography.

Group-2

Population of the second part of this study constituted of 25 subjects (9 females and 16 males, mean age 48.2 ± 17.1 years) referred at our institution for clinical CMRI examination. Among these, four patients had been referred for an evaluation of late-gadolinium enhancement after previous ST-segment elevation myocardial infarction (STEMI), 3 patients for cardiomyopathy (two hypertrophic and one dilated cardiomyopathy), one patient for a quantification of aortic steno-insufficiency in bicuspid aortic valve, one patient because of a recent onset of intermittent left bundle branch block, six patients had ventricular extrasystoles, two patients non-ST-segment elevation acute myocardial infarction and two patients acute myocarditis.

Finally six subjects were athletes referred from the Sports Medicine Unit of our Hospital for an evaluation of cardiac volumes and myocardial wall thickness because of echocardiographic or ECG findings suspicious for cardiomyopathy, which then turned out to be normal after CMRI.

We included only patients able to undergo clinical CMRI. In particular, breath-hold capability and extrasystoles had to consent to obtain adequate cine images.

The study was approved by the local ethics committee, and written informed consent was obtained from all subjects.

CMRI examination

All CMR exams were performed using a 1.5T MR system (MAGNETOM Avanto, Siemens Healthcare, Erlangen, Germany) equipped with 45 mT/m gradients and a phased-array six-channel body matrix coil together with six channels from an integrated 24-element spine matrix coil. For morphological assessment, we used an axial black-blood HASTE sequence [repetition time (TR) = 1000 ms, echo time (TE) = 28 ms, slice thickness = 8 mm]. Cine images of the heart were acquired in the two-chamber (2ch) and four-chamber (4ch) views of the left ventricle and in short-axis view (a stack of 8–14 slices from atrioventricular plane to the apex), using a TrueFISP sequence (TR = 2.5 ms, TE = 1.2 ms, slice thickness = 8 mm).

T1 and T2 mapping were obtained using a Siemens Works-In-Progress (WIP # 448, system software version VB 17A).

T1 mapping was performed utilizing a Modified Look- Locker Inversion recovery (MOLLI) pulse sequence. The standard version of the sequence that was used [2, 3] acquired 11 images over 17 heart beats resulting in a 3-3-5 pattern (three images in the first two Look-Locker segments and five images for the third inversion, with three heartbeats between acquisitions). Other pulse sequence parameters were as follows: TE/TR = 1.14/2.5 ms, flip angle 35°, matrix 124 9 192, typical in plane resolution 2.2 mm 9 1.8 mm, typical field of view 380 9 273 mm, slice thickness 8 mm, iPAT factor (GRAPPA) 2. In order to minimize off-resonance effects, patient-specific B0 shimming was performed [28].

A T2-prepared TrueFISP sequence, previously described in detail [1], was used to generate T2 maps. Pulse sequence parameters were as follows: T2 preparation time 0, 24, and 55 ms, TR = 4 9 R–R, flip angle 70°, matrix 126 9 192, typical in plane resolution 2.2 mm 9 1.8 mm, typical field of view 380 9 276 mm, slice thickness 6 mm, iPAT factor (GRAPPA) 2.

In order to generate T1 maps, the acquired inversion recovery images with different inversion times (TIs) were non-rigidly coregistered using a motion correction algorithm which is based on estimating synthetic images presenting contrast changes similar to the acquired images. In particular, the synthetic images were obtained by solving a variational energy minimization problem [29]. Then, T1 maps were estimated voxelwise by fitting a three parameter (A, B, T1*) non-linear curve [S(TI) = A – B 9 exp(–TI/T1*)] to motion corrected inversion recovery images [S(TI)] and performing a Look-Locker correction, [T1 = T1* 9 (B/A – 1)] where T1* is the apparent T1, as described in [30]. In order to generate T2 maps, a fast non-rigid registration algorithm is utilized to compensate for in-plane motion between T2-weighted images. Then, a voxelwise two parameter (M, T2) fit of motion corrected T2-weighted images [S(TE_{T2P})] with different T2 preparation times (TE_{T2P}) was performed assuming mono-exponential signal decay [S(TE_{T2P}) = M 9 exp(–TE_{T2P}/T2)] [1].

In group-1, T1 and T2 maps were acquired in diastole in three short-axis views at basal, mid-ventricular and apical levels, as well as in 4ch and 2ch view of the left ventricle.

In group-2, T1 and T2 maps were acquired both in diastole and in systole (Fig. 1). In preliminary tests, three experienced readers (CT, JDM, LS) evaluated the ideal delay time for image acquisition at systole. By consensus, a delay time of 150 ms after the R-wave was judged to provide a good image quality for T2 maps. For T1 maps, the minimum delay time allowed by the standard MOLLI sequence was utilized (~330 ms).

CMRI image analysis

Ventricular function

TrueFISP cine images were visually evaluated regarding wall motion abnormalities. The quantification of left-ventricular function, volumes and mass was performed using the Argus Ventricular Function software (Siemens Healthcare). All volumes and mass were indexed to body surface area.

T1 and T2 mapping: qualitative assessment

T1-/T2-weighted source images as well as T1/T2 maps were assessed regarding artifacts due to off-resonance effects (susceptibility and B0-field inhomogeneities artifacts), cardiac or respiratory motion. The presence of artifacts led to the exclusion of all affected myocardial segments from further analysis. Three experienced readers (CT, JDM, LS) assessed artifacts in consensus. In the group-2, plainly pathologic segments, and signally segments displaying edema, late-gadolinium enhancement or a-dyskinesia, were excluded from analysis, both in order to obtain homogeneous T1 and T2 values that enabled to identify out-of-range measures as artifacts and because akinetic segments are not expected to show a systolic increase of wall thickness.

T1 and T2 mapping: quantitative assessment

T1 and T2 maps were divided into myocardial segments according to the standard 17-segment model recommended by the American College of Cardiology/American Heart Association [31]. We excluded from data analysis the true apex (i.e. the segment number 17), given that it is characterized by unavoidable partial-volume effect [1, 2]. Depending on the wall thickness, an experienced reader (NL) drew a 3 9 3 or 2 9 2 pixels ROI on the T1/T2 maps in each of the remaining 16 segments, and the mean value of T1/T2 within each ROI was recorded.

The window setting was individually adjusted for each map in order to display any partial-volume effect and to avoid inclusion of blood/tissue adjacent to myocardial wall.

Overall myocardial T1/T2 values were calculated by averaging the segment T1/T2 values across all 16 segments in short-axis view. In addition, regional myocardial T1/T2 values were calculated by averaging the segment T1/T2 values across the basal, mid-ventricular and apical segments in short-axis, 4ch and 2ch views.

In order to assess intra-observer variability, in fifteen patients of group-2 the reader (NL) performed ROI T1/T2 measurements, for both diastolic and systolic acquisitions, in the short-axis view in two distinct sessions, at least 1 month apart. Also, in order to assess inter-observer variability, a second experienced reader (CT), blinded to the

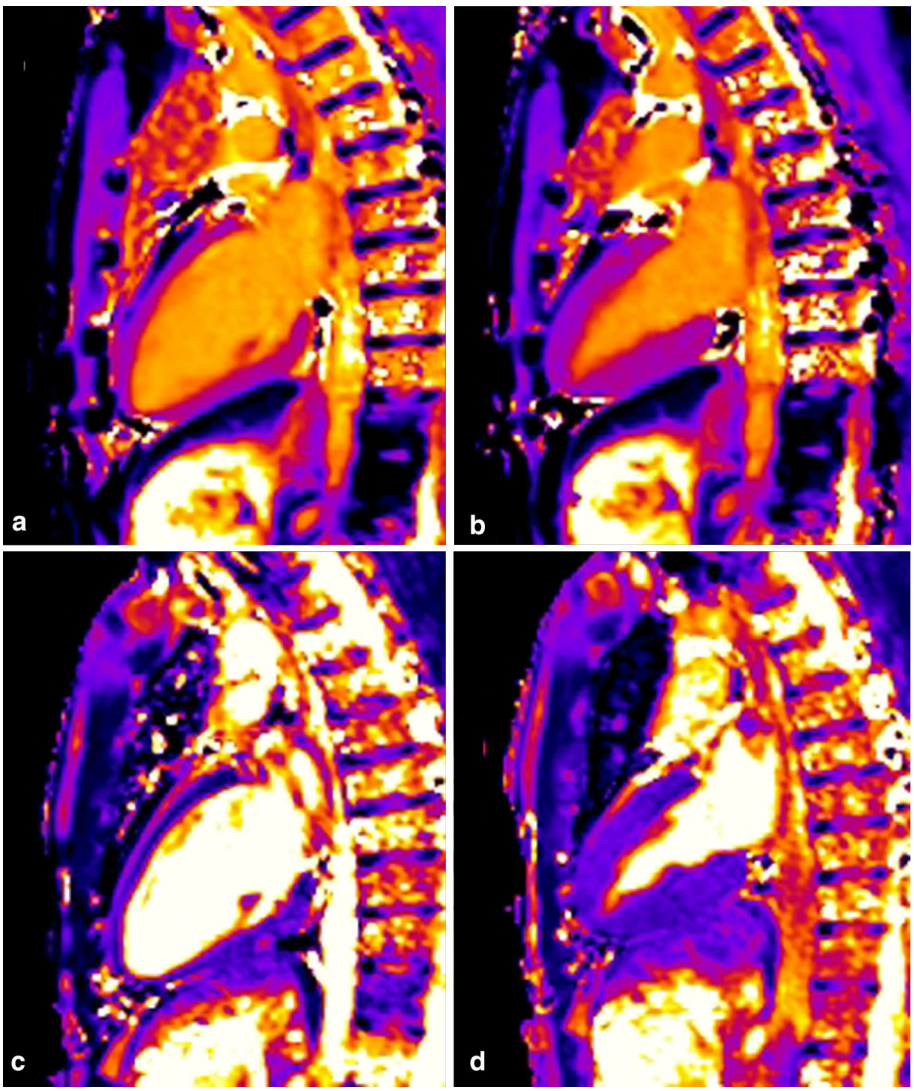

Fig. 1 Diastolic and systolic T1 and T2 maps. T1 (a, b) and T2 (c, d) maps acquired in 2ch view of left ventricle in diastole (a, c) and in systole (b, d). In systole the increased myocardial wall thickness is expected to reduce partial-volume effects

assessment of the first reader, repeated the ROI T1/T2 measurements in the short-axis view.

Statistical analysis

Group-1

For all views (short-axis, 4ch and 2ch views), comparisons of regional (basal, mid-ventricular and apical segments) T1/T2 values were performed through a repeated measures ANOVA with Tukey's multiple comparison test. For all tests, a p value \0.05 was considered statistically significant.

Group-2

For all views (short-axis, 4ch and 2ch views) as well as for both diastole and systole datasets, comparisons of regional (basal, mid-ventricular and apical segments) T1/T2 values were performed through a repeated measures ANOVA with Tukey's multiple comparison test. For all regions (basal, mid-ventricular and apical segments) differences in regional T1/T2 values between diastole and systole were assessed through a paired t test. Intra- and inter-observer variability of T1/T2 measures in diastole and systole for short-axis view was assessed by using the Bland-and-Altman method with computation of the mean difference and 95 % limits of agreement (LoAs) [32].

For all tests, a p value \0.05 was considered statistically significant.

Results

Group-1

In T1 maps, from 616 segments 84.6 % were judged eligible for analysis, while 15.4 % had to be discarded due to off-resonance and motion artifacts (3.7 %), to unavoidable partial-volume effects because of a relatively low wall thickness with respect to the size of the ROI (6.3 %) or both (5.4 %; Fig. 2). The majority of excluded segments (85.3 %) were located at apical level. In T2 maps, 0.8 % of segments were judged not eligible for analysis due to partial-volume effect (Table 1).

At least in one plane, 10 (45 %) out of 22 healthy volunteers had all 16 segments evaluable in T1 maps, while 21 subjects (95 %) had all segments evaluable in T2 maps.

Mean of T1/T2 values in short-axis, 4ch and 2ch views are detailed in Table 2.

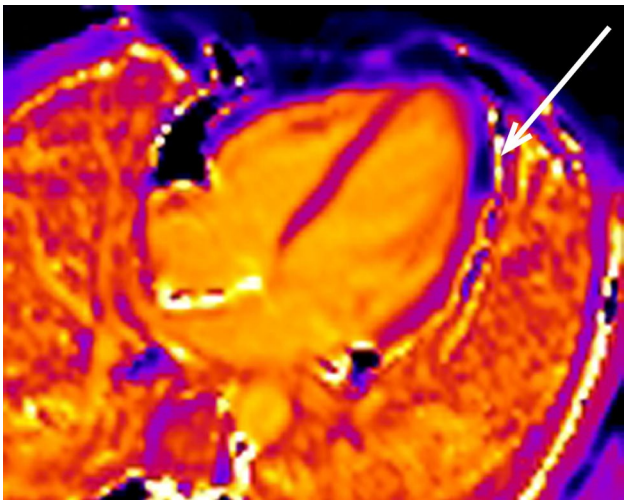

Fig. 2 Artifacts in T1 maps. Modified Look-Locker inversion recovery (MOLLI) sequence acquired in 4ch view in diastole; severe off-resonance artifacts (*arrow*) prevent a reliable evaluation of the lateral wall of left ventricle at apical level

Table 1 Percentage of invaluable segments at basal, mid-ventricular and apical levels

	Basal (%)	Mid (%)	Apical (%)	Overall (%)
Group-1				
T1	0.3	2.0	13.1	15.4
T2	0.3	0.0	0.5	0.8
Group-2				
T1 in diastole	2.8	6.4	11.9	21.1
T1 in systole	2.3	0.6	2.3	5.3
T2 in diastole	1.4	2.0	0.6	4.0
T2 in systole	0.5	0.3	0.0	0.8

For all views, we found no significant difference in regional T1 values among basal, mid-ventricular or apical segments in short-axis ($p = 0.39$), 4ch ($p = 0.67$) and2ch ($p = 0.16$) views.

Mean T2 values in apical segments were significantly higher than mean T2 values measured at basal and mid- ventricular levels for short-axis (p \ 0.0001) as well as 4ch (p \ 0.009) and 2ch views ($p = 0.0002$) (Table 3).

Group-2

Forty-seven out of 700 segments (6.7 %) were pathologic at visual evaluation and therefore were discarded from further analyses. One-hundred and thirty-eight segments out of the remaining 653 segments (21.1 %), mainly located at apical levels, were judged not eligible for analysis when T1 maps were obtained in diastole, while 5.3 % segments were discarded when T1 maps were obtained in systole (Table 1).

Due to partial-volume effect, 4.0 and 0.8 % of segments were invaluable in T2 maps obtained in diastole and systole, respectively (Table 1).

At least in one plane and excluding pathologic segments discarded from analysis, 24 %/72 % of patients had all segments evaluable in diastolic/systolic T1 maps, while 60 %/84 % of patients had all segments evaluable in diastolic/systolic T2 maps, respectively.

In maps acquired in diastole there were no significant differences in T1 values across short-axis slices ($p = 0.40$) nor among basal, mid-ventricular and apical segments in 4ch view ($p = 0.60$) and in 2ch view ($p = 0.17$; Table 2). For acquisitions in diastole, apical T2 values were significantly higher than basal and mid-ventricular T2 values in short-axis ($p \setminus 0.0001$) as well as in 4ch ($p \setminus 0.0001$) and 2ch ($p \setminus 0.0001$) views (Table 2).

For acquisitions in systole, there was no significant difference in T1 and T2 values among basal, mid-ventricular and apical segments in short-axis (T1, $p = 0.93$; T2, $p = 0.37$), in 4ch (T1, $p = 0.42$; T2, $p = 0.29$) and in 2ch views (T1, $p = 0.19$; T2, $p = 0.71$).

In short-axis (52.3 vs 56.1 ms, $p \setminus 0.0001$), 4ch (52.8 vs 56.5, $p = 0.001$) and 2ch views (53.0 vs 58.9 ms, $p \setminus 0.0001$), apical T2 values were significantly lower in maps obtained in systole with respect to those obtained in diastole. No other significant difference was found between systolic and diastolic T1/T2 maps.

Intra- and inter-observer variability was low; mean difference and 95 % limits of agreement are detailed in Table 4.

Discussion

This study involved a systematic in vivo assessment of the distribution of overall quality of cardiac T1 and T2 maps among myocardial segments. We found that cardiac T1 and T2 maps show relevant artifacts in apical segments, which are likely due to the reduced myocardial wall thickness at these levels. Also, the acquisition in systole does not cause more artifacts than the acquisition in diastole and increases the number of the evaluable segments.

Myocardial T1 and T2 values reported in the literature vary substantially with field strength as well as the specific method and imaging protocol utilized. Hence, there is general consensus that it is necessary to generate reference values specific for each site, technique and imaging setting [28]. The T1 and T2 obtained in our study are in agreement with T1 and T2 values reported in previous studies which have employed the same sequences at 1.5T [1, 2, 26].

Accordingly to the results of previous studies [1, 23], when visually evaluated, cardiac T2 maps obtained in diastole resulted adequate in the vast majority of the cases (99.2 %/96 % of myocardial segments in group-1/group-2, respectively). On the contrary, in healthy volunteers (group-1) an unexpected high number (15.4 %) of myocardial segments, mainly located at apical level (85.3 %), showed relevant artifacts and were judged invaluable in T1 maps, and this finding was confirmed in the group of patients (group-2, 21.1 % of segments).

Therefore, despite in the present study some of the segments have been evaluated in more than one plane, a high percentage of subjects had non-evaluable segments in T1 maps, in particular when the maps were obtained in diastole.

Table 2 T1 and T2 measures of group-1 and group-2 in short-axis, 4ch and 2ch views (mean ± standard deviation)

	Group-1		Group-2 (diastole)		Group-2 (systole)	
	T1 (ms)	T2 (ms)	T1 (ms)	T2 (ms)	T1 (ms)	T2 (ms)
Short-axis view						
Overall	960.6 ± 27.5	52.6 ± 2.4	963.3 ± 40.4	53.0 ± 2.4	957.0 ± 33.1	52.1 ± 2.3
Basal level	979.8 ± 31.0	51.2 ± 2.3	956.8 ± 35.6	51.3 ± 2.4	954.4 ± 34.1	52.3 ± 2.7
Mid-ventricular level	956.1 ± 57.0	52.5 ± 2.6	965.5 ± 49.2	52.2 ± 2.6	956.0 ± 37.6	51.6 ± 2.3
Apical level	967.5 ± 61.2	58.2 ± 4.4	973.7 ± 62.8	56.1 ± 4.2*	953.4 ± 50.8	52.3 ± 2.6§
4ch view						
Basal level	946.0 ± 20.8	49.9 ± 2.5	961.5 ± 50.5	51.0 ± 2.9	959.8 ± 47.5	50.4 ± 1.8
Mid-ventricular level	939.1 ± 40.1	49.8 ± 2.6	945.9 ± 52.6	51.6 ± 2.8	947.3 ± 42.7	52.0 ± 2.6
Apical level	937.3 ± 65.9	53.0 ± 4.9	952.8 ± 61.6	56.5 ± 6.1*	951.0 ± 56.3	52.8 ± 5.0^
2ch view						
Basal level	964.4 ± 52.2	51.2 ± 3.0	964.2 ± 57.3	52.5 ± 3.1	948.8 ± 30.8	52.5 ± 4.0
Mid-ventricular level	994.2 ± 42.0	51.2 ± 2.9	958.5 ± 57.3	52.2 ± 2.3	961.7 ± 44.9	52.0 ± 2.5
Apical level	978.3 ± 53.0	53.8 ± 4.0	953.6 ± 61.5	58.9 ± 5.1*	958.9 ± 51.1	53.0 ± 3.1§

* $p \setminus 0.0001$ versus basal and mid-ventricular level (repeated measures ANOVA with Tukey's multiple comparison test)

§ $p \setminus 0.0001$ versus diastole (paired *t* test)

^ $p = 0.001$ versus diastole (paired *t* test)

Table 3 Results of repeated measures ANOVA with Tukey's multiple comparison test of regional T2 values (basal, mid-ventricular and apical levels) in a group of healthy subjects (group-1)

Comparison between levels	Mean difference (ms)	95 % CI of difference (ms)	Multiplicity adjusted *p* value
Short-axis view			
Basal versus Mid-ventricular	−1.359	−3.186 to 0.4675	0.18
Basal versus Apical	−6.973	−8.799 to −5.146	\0.0001*
Mid-ventricular versus Apical	−5.614	−7.440 to −3.787	\0.0001*
4ch view			
Basal versus Mid-ventricular	0.1682	−2.016 to 2.352	0.98
Basal versus Apical	−3.086	−5.270 to 0.9025	0.0038*
Mid-ventricular versus Apical	−3.255	−5.438 to −1.071	0.0022*
2ch view			
Basal versus Mid-ventricular	−0.04545	−1.631 to 1.540	0.997
Basal versus Apical	−2.645	−4.231 to −1.060	0.0006*
Mid-ventricular versus Apical	−2.6	−4.185 to –1.015	0.0008*

* Significant (multiplicity adjusted value $p \setminus 0.05$)

In a recent study in 40 young healthy volunteers, in which a MOLLI sequence with a different sampling scheme (5-2 pattern) was utilized, only 1.2 % of segments were qualitatively judged as non-evaluable because of artifacts or partial-volume effect due to their proximity to the left ventricular outflow tract [27].

In this study, we applied the standard MOLLI sequence (3-3-5 pattern) introduced by Messroghli et al. [2]. In their study in 15 healthy subjects, 4.3 % of segments were considered as non-evaluable, mainly because of respiratory or ventricular motion, while in a 3T study in 60 healthy subjects [23], in which the same MOLLI acquisition scheme was utilized, 8.4 % of segments were excluded, mainly because of off-resonance artifacts.

Table 4 Results of Bland-and-Altman method: mean difference and 95 % limits of agreement for intra- and inter-operator measurements

	Mean difference (%)	95 % limits of agreement
Intra-operator		
T1 in diastole	0.8	from −3.8 to 5.5 %
T1 in systole	−0.5	from −6.0 to 5.0 %
T2 in diastole	0.4	from −4.0 to 4.7 %
T2 in systole	−0.7	from −5.8 to 4.3 %
Inter-operator		
T1 in diastole	−0.3	from −5.4 to 4.8 %
T1 in systole	0.4	from −4.5 to 5.2 %
T2 in diastole	−1.2	from −7.0 to 4.6 %
T2 in systole	−0.4	from −8.4 to 7.6 %

We found both off-resonance artifacts and artifacts related to cardiac or respiratory motion, that we judged problematic especially in the apical regions where they prevented us to place the ROIs because of the reduced myocardial wall thickness at that level. As a whole, our results suggest that native (noncontrast) T1 maps are more prone to artifacts than T2 maps, when all myocardial regions are visually scrutinized, and that a comprehensive evaluation of the left ventricle is more challenging in T1 than T2 maps.

Previous studies provided conflicting results regarding the variability of T1 and T2 values among myocardial segments. Some authors [2, 16] found no significant difference in T1 measures across the 16 segments of the left ventricle. However, others have reported an increase of T1 and T2 values from base to apex [23], higher T1 values in septal myocardium with respect to lateral segments [27], higher T2 values in apical segments with respect to those measured at basal and mid-ventricular levels [1, 33], and higher T2 values in anteroseptal segments compared to posterolateral segments [33].

In our cohort, there were no regional differences in myocardial T1 values. However, we discarded from analysis a high number of apical segments, and this is likely to have influenced the results. On the other hand, we found that T2 values in apical segments were significantly higher with respect to those measured at basal and mid-ventricular levels, and this suggests that, also in maps appearing free from relevant artifacts at visual evaluation, T2 values measured in apical segments could be actually biased by partial-volume effect due to the inclusion of cavity blood into the ROI. Accordingly, in a study in 73 healthy volunteers [24], T2 values were inversely correlated to myocardial wall thickness. These results seem to suggest that partial-volume effect might contribute to explain the differences in T1 and T2 values among myocardial segments reported in some of the previous studies.

In order to limit the potential error due to partial-volume effect, it has been proposed to use one pixel erosion to represent ‘‘mid-wall myocardial’’ T1 [25]. However, this method could be difficult to apply for lower myocardial thickness, as in the apex.

Therefore, although the maps are generally obtained at end diastole, given that the myocardium is thicker during systole, it could be advantageous to obtain T1 and T2 maps in this cardiac phase in order to reduce partial-volume effect. In maps obtained in systole, an increase of artifacts, due to motion both during acquisition of single source images as well as among source images, could be expected. However, a few pilot studies in healthy subjects have demonstrated that T1 mapping is feasible also in systole while, to the best of our knowledge, so far no study has thoroughly evaluated systolic T2 maps. In a 3T study [17], MOLLI sequences were acquired in mid-ventricular short-axis view in both diastole and systole, before and after administration of gadolinium. These authors found that, contrary to the general opinion, maps obtained at early systole resulted in a constantly good quality, even slightly better than the quality of the maps obtained in diastole. In another study [26], T1 mapping of the right ventricle has proven to be feasible in systole in 18 out of 20 healthy subjects, although only with a small ROI, at least in one of the three slices acquired (mid-ventricular short-axis view, 4ch view and transversal plane), while in diastole the myocardial thickness was too low to consent reliable measurements. Finally, Reiter et al. [27] have obtained T1 maps in three short-axis

slices at basal, mid-ventricular and apical levels at both early systole and late diastole, showing that acquisitions in systole and in diastole were characterized by a similar image quality at visual evaluation.

Our findings confirm that the acquisition in systole does not cause an increase of the artifacts when compared to more usually performed diastolic acquisition, and, on the contrary, reduce the number of invaluable myocardial segments in T1 maps. Furthermore, in maps obtained in systole the differences in measured T2 values between apical segments and mid-ventricular and basal segments that we found in diastole are no longer detectable, possibly because of a reduction of partial-volume effect.

Previous studies have reported different T1 values of myocardium between systole and diastole. In particular, Kawel et al. [17], have shown that myocardial T1 at 3T was 1 % shorter in systole when compared to diastole pre-contrast, and 2 % shorter in diastole when compared to systole post-contrast. Also, in the 1.5T study by Reiter et al. [27], diastolic values of T1 were about 2 % greater than systolic T1 values. Therefore, it is recommended to obtain T1 measurements in the same cardiac phase in order to avoid potential bias [28].

These differences have been related to the changes in myocardial blood volume between systole and diastole demonstrated both in ex vivo and in vivo studies [34–36], that in theory are expected to influence both T1 and T2 values. Nonetheless, as previously suggested [37], an additional contributing factor could be the partial-volume effect at the edge of the myocardium, which is more relevant in thinner myocardium during diastole than during systole. However, the revealed differences in myocardial relaxation times were fairly small in absolute values, being comprised between 5 and 25 ms in the abovementioned studies, and their clinical relevance remains to be assessed in greater detail.

In this study, no significant difference in myocardial relaxation times between systolic and diastolic phase was revealed, except the increase of T2 values in apical segments in diastole which is likely to be due to partial-volume effect. We can tentatively submit that a higher number of subjects might have been necessary to unveil such small absolute differences.

We recognize as potential limitation of this study the employment of fairly small ROIs with size less than that (10 pixels) usually suggested in order to reduce the influence of noise when employing either black blood STIR or fast spin-echo T2-weighted sequences for the evaluation of myocardial edema [38]. However, the use of ROIs with larger size would have further increased partial-volume effect, especially in apical segments. Furthermore, our fairly small ROIs evaluate only a subsample of the corresponding segment. However, given that T1/T2 values are expected to be spatially uniform within a myocardial segment without pathologic changes, the measured T1/T2 can be considered as representative of the values of the segment avoiding the inclusion of potential artifacts. For T1 and T2 mapping, we used the standard version of the prototype MOLLI and T2-TrueFISP sequences provided by the scanner vendor. Acquisition sequences with improved spatial resolution might be advantageous to reduce partial-volume effect.

Furthermore, the systolic maps of relaxation times were acquired at fixed delays times after the R wave, that differed between T1 and T2 maps. We chose the allowed delay times that we judged to produce the better image quality in the standard sequences utilized, resulting in agreement with the delay times employed in other studies [17, 27]. Nonetheless, it is possible that a delay time tailored on the individual R–R interval might further improve the overall quality of T1/T2 maps.

Conclusions

When myocardial T1 and T2 mapping are performed in diastole, the quality of the maps is not homogeneous among myocardial segments. In particular apical segments, as compared to segments at basal and mid-ventricular levels, are more prone to artifacts, and this could be problematic when evaluating focal myocardial changes. The acquisition in systole does not cause an increase of artifacts and, on the contrary, increases the number of evaluable segments.

References

1. Giri S, Chung YC, Merchant A, Mihai G, Rajagopalan S, Raman SV, Simonetti OP (2009) T2 quantification for improved detection of myocardial edema. J Cardiovasc Magn Reson Off J Soc Cardiovasc Magn Reson 11:56. doi:10.1186/1532-429X-11-56
2. Messroghli DR, Plein S, Higgins DM, Walters K, Jones TR, Ridgway JP, Sivananthan MU (2006) Human myocardium: single-breath-hold MR T1 mapping with high spatial resolution—reproducibility study. Radiology 238(3):1004–1012. doi:10.1148/radiol.2382041903
3. Messroghli DR, Radjenovic A, Kozerke S, Higgins DM, Sivananthan MU, Ridgway JP (2004) Modified Look-Locker inversion recovery (MOLLI) for high-resolution T1 mapping of the heart. Magn Reson Med Off J Soc Magn Reson Med 52(1):141–146. doi:10.1002/mrm.20110
4. Park CH, Choi EY, Kwon HM, Hong BK, Lee BK, Yoon YW, Min PK, Greiser A, Paek MY, Yu W, Sung YM, Hwang SH, Hong YJ, Kim TH (2013) Quantitative T2 mapping for detecting myocardial edema after reperfusion of myocardial infarction: validation and comparison with T2-weighted images. Int J Cardiovasc Imaging 29(Suppl 1):65–72. doi:10.1007/s10554-013-0256-0
5. Verhaert D, Thavendiranathan P, Giri S, Mihai G, Rajagopalan S, Simonetti OP, Raman SV (2011) Direct T2 quantification of myocardial edema in acute ischemic injury. JACC Cardiovasc Imaging 4(3):269–278. doi:10.1016/j.jcmg.2010.09.023
6. Zia MI, Ghugre NR, Connelly KA, Strauss BH, Sparkes JD, Dick AJ, Wright GA (2012) Characterizing myocardial edema and hemorrhage using quantitative T2 and T2* mapping at multiple time intervals post ST-segment elevation myocardial infarction. Circ Cardiovasc Imaging 5(5):566–572. doi:10.1161/CIRCIMAGING.112.973222
7. Ferreira VM, Piechnik SK, Dall'Armellina E, Karamitsos TD, Francis JM, Ntusi N, Holloway C, Choudhury RP, Kardos A, Robson MD, Friedrich MG, Neubauer S (2013) T(1) mapping for the diagnosis of acute myocarditis using CMR: comparison to T2-weighted and late gadolinium enhanced imaging. JACC Cardiovasc Imaging 6(10):1048–1058. doi:10.1016/j.jcmg.2013.03.008
8. Thavendiranathan P, Walls M, Giri S, Verhaert D, Rajagopalan S, Moore S, Simonetti OP, Raman SV (2012) Improved detection of myocardial involvement in acute inflammatory cardiomyopathies using T2 mapping. Circ Cardiovasc Imaging 5(1):102–110. doi:10.1161/CIRCIMAGING.111.967836
9. Ferreira VM, Piechnik SK, Dall'Armellina E, Karamitsos TD, Francis JM, Choudhury RP, Friedrich MG, Robson MD, Neubauer S (2012) Non-contrast T1-mapping detects acute myocardial edema with high diagnostic accuracy: a comparison to T2- weighted cardiovascular magnetic resonance. J Cardiovasc Magn Reson Off J Soc Cardiovasc Magn Reson 14:42. doi:10.1186/1532-429X-14-42
10. Bull S, White SK, Piechnik SK, Flett AS, Ferreira VM, Loudon M, Francis JM, Karamitsos TD, Prendergast BD, Robson MD, Neubauer S, Moon JC, Myerson SG (2013) Human non-contrast T1 values and correlation with histology in diffuse fibrosis. Heart 99(13):932–937. doi:10.1136/heartjnl-2012-303052
11. Flett AS, Hayward MP, Ashworth MT, Hansen MS, Taylor AM, Elliott PM, McGregor C, Moon JC (2010) Equilibrium contrast cardiovascular magnetic resonance for the measurement of diffuse myocardial fibrosis: preliminary validation in humans. Circulation 122(2):138–144. doi:10.1161/CIRCULATIONAHA.109.930636
12. Banypersad SM, Sado DM, Flett AS, Gibbs SD, Pinney JH, Maestrini V, Cox AT, Fontana M, Whelan CJ, Wechalekar AD, Hawkins PN, Moon JC (2013) Quantification of myocardial extracellular volume fraction in systemic AL amyloidosis: an equilibrium contrast cardiovascular magnetic resonance study. Circ Cardiovasc Imaging 6(1):34–39. doi:10.1161/CIRCIMAGING.112.978627
13. Fontana M, Banypersad SM, Treibel TA, Maestrini V, Sado DM, White SK, Pica S, Castelletti S, Piechnik SK, Robson MD, Gilbertson JA, Rowczenio D, Hutt DF, Lachmann HJ, Wechalekar AD, Whelan CJ, Gillmore JD, Hawkins PN, Moon JC (2014) Native T1 mapping in transthyretin amyloidosis. JACC Cardiovasc Imaging 7(2):157–165. doi:10.1016/j.jcmg.2013.10.008
14. Karamitsos TD, Piechnik SK, Banypersad SM, Fontana M, Ntusi NB, Ferreira VM, Whelan CJ, Myerson SG, Robson MD, Hawkins PN, Neubauer S, Moon JC (2013) Noncontrast T1 mapping for the diagnosis of cardiac amyloidosis. JACC Cardiovasc Imaging 6(4):488–497. doi:10.1016/j.jcmg.2012.11.013
15. Robbers LF, Baars EN, Brouwer WP, Beek AM, Hofman MB, Niessen HW, van Rossum AC, Marcu CB (2012) T1 mapping shows increased extracellular matrix size in the myocardium due to amyloid depositions. Circ Cardiovasc Imaging 5(3):423–426. doi:10.1161/CIRCIMAGING.112.973438
16. Chin CW, Semple S, Malley T, White AC, Mirsadraee S, Weale PJ, Prasad S, Newby DE, Dweck MR (2014) Optimization and comparison of myocardial T1 techniques at 3T in patients with aortic stenosis. Eur Heart J Cardiovasc Imaging 15(5):556–565. doi:10.1093/ehjci/jet245
17. Kawel N, Nacif M, Zavodni A, Jones J, Liu S, Sibley CT, Bluemke DA (2012) T1 mapping of the myocardium: intra-individual assessment of the effect of field strength, cardiac cycle and variation by myocardial region. J Cardiovasc Magn Reson Off J Soc Cardiovasc Magn Reson 14:27. doi:10.1186/1532-429X-14-27

18. Kellman P, Arai AE, Xue H (2013) T1 and extracellular volume mapping in the heart: estimation of error maps and the influence of noise on precision. J Cardiovasc Magn Reson Off J Soc Cardiovasc Magn Reson 15:56. doi:10.1186/1532-429X-15-56
19. Kellman P, Hansen MS (2014) T1-mapping in the heart: accuracy and precision. J Cardiovasc Magn Reson Off J Soc Cardiovasc Magn Reson 16:2. doi:10.1186/1532-429X-16-2
20. Kellman P, Herzka DA, Arai AE, Hansen MS (2013) Influence of Off-resonance in myocardial T1-mapping using SSFP based MOLLI method. J Cardiovasc Magn Reson Off J Soc Cardiovasc Magn Reson 15:63. doi:10.1186/1532-429X-15-63
21. Raman FS, Kawel-Boehm N, Gai N, Freed M, Han J, Liu CY, Lima JA, Bluemke DA, Liu S (2013) Modified look-locker inversion recovery T1 mapping indices: assessment of accuracy and reproducibility between magnetic resonance scanners. J Cardiovasc Magn Reson Off J Soc Cardiovasc Magn Reson 15:64. doi:10.1186/1532-429X-15-64
22. Roujol S, Weingartner S, Foppa M, Chow K, Kawaji K, Ngo LH, Kellman P, Manning WJ, Thompson RB, Nezafat R (2014) Accuracy, precision, and reproducibility of four T1 mapping sequences: a head-to-head comparison of MOLLI, ShMOLLI, SASHA, and SAPPHIRE. Radiology 272(3):683–689. doi:10.1148/radiol.14140296
23. von Knobelsdorff-Brenkenhoff F, Prothmann M, Dieringer MA, Wassmuth R, Greiser A, Schwenke C, Niendorf T, Schulz- Menger J (2013) Myocardial T1 and T2 mapping at 3 T: reference values, influencing factors and implications. J Cardiovasc Magn Reson Off J Soc Cardiovasc Magn Reson 15:53. doi:10.1186/1532-429X-15-53
24. Wassmuth R, Prothmann M, Utz W, Dieringer M, von Knobelsdorff-Brenkenhoff F, Greiser A, Schulz-Menger J (2013) Variability and homogeneity of cardiovascular magnetic resonance myocardial T2-mapping in volunteers compared to patients with edema. J Cardiovasc Magn Reson Off J Soc Cardiovasc Magn Reson 15:27. doi:10.1186/1532-429X-15-27
25. Piechnik SK, Ferreira VM, Lewandowski AJ, Ntusi NA, Banerjee R, Holloway C, Hofman MB, Sado DM, Maestrini V, White SK, Lazdam M, Karamitsos T, Moon JC, Neubauer S, Leeson P, Robson MD (2013) Normal variation of magnetic resonance T1 relaxation times in the human population at 1.5 T using ShMOLLI. J Cardiovasc Magn Reson Off J Soc Cardiovasc Magn Reson 15:13. doi:10.1186/1532-429X-15-13
26. Kawel-Boehm N, Dellas Buser T, Greiser A, Bieri O, Bremerich J, Santini F (2014) In-vivo assessment of normal T1 values of the right-ventricular myocardium by cardiac MRI. Int J Cardiovasc Imaging 30(2):323–328. doi:10.1007/s10554-013-0326-3
27. Reiter U, Reiter G, Dorr K, Greiser A, Maderthaner R, Fuchsjager M (2014) Normal diastolic and systolic myocardial T1 values at 1.5-T MR imaging: correlations and blood normalization. Radiology 271(2):365–372. doi:10.1148/radiol.13131225
28. Moon JC, Messroghli DR, Kellman P, Piechnik SK, Robson MD, Ugander M, Gatehouse PD, Arai AE, Friedrich MG, Neubauer S, Schulz-Menger J, Schelbert EB, Society for Cardiovascular Magnetic Resonance I, Cardiovascular Magnetic Resonance Working Group of the European Society of C (2013) Myocardial T1 mapping and extracellular volume quantification: a Society for Cardiovascular Magnetic Resonance (SCMR) and CMR Working Group of the European Society of Cardiology consensus statement. J Cardiovasc Magn Reson Off J Soc Cardiovasc Magn Reson 15:92. doi:10.1186/1532-429X-15-92
29. Xue H, Shah S, Greiser A, Guetter C, Littmann A, Jolly MP, Arai AE, Zuehlsdorff S, Guehring J, Kellman P (2012) Motion correction for myocardial T1 mapping using image registration with synthetic image estimation. Magn Reson Med Off J Soc Magn Reson Med 67(6):1644–1655. doi:10.1002/mrm.23153
30. Messroghli DR, Greiser A, Frohlich M, Dietz R, Schulz-Menger J (2007) Optimization and validation of a fully-integrated pulse sequence for modified look-locker inversion-recovery (MOLLI) T1 mapping of the heart. J Magn Reson Imaging JMRI 26(4):1081–1086. doi:10.1002/jmri.21119
31. Cerqueira MD, Weissman NJ, Dilsizian V, Jacobs AK, Kaul S, Laskey WK, Pennell DJ, Rumberger JA, Ryan T, Verani MS, American Heart Association Writing Group on Myocardial S, Registration for Cardiac I (2002) Standardized myocardial seg- mentation and nomenclature for tomographic imaging of the heart. A statement for healthcare professionals from the Cardiac Imaging Committee of the Council on Clinical Cardiology of the American Heart Association. Circulation 105(4):539–542
32. Bland MJ, Altman DG (1986) Statistical methods for assessing agreement between two methods of clinical measurements. Lancet 327(8476):307–310. doi:10.1016/S0140-6736(86)90837-8
33. Bonner F, Janzarik N, Jacoby C, Spieker M, Schnackenburg B, Range F, Butzbach B, Haberkorn S, Westenfeld R, Neizel-Wittke M, Flogel U, Kelm M (2015) Myocardial T2 mapping reveals age- and sex-related differences in volunteers. J Cardiovasc Magn Reson Off J Soc Cardiovasc Magn Reson 17(1):9. doi:10.1186/ s12968-015-0118-0
34. Judd RM, Levy BI (1991) Effects of barium-induced cardiac contraction on large- and small-vessel intramyocardial blood volume. Circ Res 68(1):217–225
35. Toyota E, Fujimoto K, Ogasawara Y, Kajita T, Shigeto F, Mat- sumoto T, Goto M, Kajiya F (2002) Dynamic changes in three-dimensional architecture and vascular volume of transmural coronary microvasculature between diastolic-

and systolic-arrested rat hearts. Circulation 105(5):621–626
36. Wu EX, Tang H, Wong KK, Wang J (2004) Mapping cyclic change of regional myocardial blood volume using steady-state susceptibility effect of iron oxide nanoparticles. J Magn Reson Imaging JMRI 19(1):50–58. doi:10.1002/jmri.10426
37. Pattanayak P, Bluemke DA (2014) Cardiac MR imaging to probe tissue composition of the heart by using T1 mapping. Radiology 271(2):320–322. doi:10.1148/radiol.14140287
38. Friedrich MG, Sechtem U, Schulz-Menger J, Holmvang G, Alakija P, Cooper LT, White JA, Abdel-Aty H, Gutberlet M, Prasad S, Aletras A, Laissy JP, Paterson I, Filipchuk NG, Kumar A, Pauschinger M, Liu P, International Consensus Group on Cardiovascular Magnetic Resonance in M (2009) Cardiovascular magnetic resonance in myocarditis: a JACC white paper. J Am Coll Cardiol 53(17):1475–1487. doi:10.1016/j.jacc.2009.02.007